APR 1 1947

NATIONAL ADVISORY COMMITTEE FOR AERONAUTICS

TECHNICAL MEMORANDUM

No. 1123

INVESTIGATIONS ON EXPERIMENTAL IMPELLERS FOR AXIAL BLOWERS

By W. Encke

Göttingen Aerodynamic Experimental Station (AVA)
Göttingen, Germany

NACA
LANGLEY MEMORIAL AERONAUTICAL
LABORATORY
Langley Field, Va.

Washington
April, 1947

NASA Technical Library
3 1176 01441 2291

NATIONAL ADVISORY COMMITTEE FOR AERONAUTICS

TECHNICAL MEMORANDUM NO. 1123

INVESTIGATION ON EXPERIMENTAL IMPELLERS FOR AXIAL BLOWERS*

By W. Encke

Abstract: A selection of measurements obtained on experimental impellers for axial blowers will be reported. In addition to characteristic curves plotted for low and for high peripheral velocities, proportions and blade sections for six different blower models and remarks on the design of blowers will be presented.

I. Foreword:

A selection of measurements obtained on experimental impellers for axial blowers will be reported. Some of these observations are from rather old experiments. The latter led to the designing early in 1930 of a purely axial supercharger for use at an altitude of 5 kilometers; this design was planned as a five-stage axial compressor with a rotor speed of 30,000 rpm but due to the bearing difficulties then existing it was not completed.

Inasmuch as these older impellers are even today still being utilized in single-stage and multistage blowers - the oldest, rotor 866, has been used with great success quite recently in conjunction with later-designed rotors E68 and E78 for an eight-stage compressor - it is felt that the measurements made of them, supplemented by the results obtained with some additional experimental impellers, should be made available to a wider public.

II. Formulation of the Problem; Arrangement and Execution of the Experiments:

The experimental impellers discussed were designed to clarify whether it was possible to increase the pressure rise obtainable per

---

*"Untersuchungen an Modellrädern von Axialgebläsen." Aerodynamische Versuchsanstalt Göttingen E. V., Göttingen, Inst. f. Strömungsmaschinen, ZWB,M 94, Nr. 3135, April 1944, pp. 1-28.

stage considerably above the relatively small pressure differences produced up to that time in axial blowers, the desire being to come out with a relatively small number of rotors in the process of attaining a prescribed rather large pressure ratio by placing several rotors in tandem. The ultimate goal foreseen was the design of the blading of a multistage axial compressor for supercharging high-altitude aircraft engines (reference 1).

Keeping in mind the limit placed by the Mach number on the increase of the relative air velocity, the first step in developing the blower was to attempt to increase the pressure rise obtainable per rotor substantially above existing limits by means of appropriate shaping of the impeller blades. Next to be investigated was how far the rotor peripheral speed could be increased toward the point at which the relative air velocity would equal the speed of sound, with the purpose of maintaining a good degree of efficiency while securing the highest possible pressure increases. Further studies were then to be made on the problem of reducing the then very great longitudinal dimensions of axial blowers without any important loss in efficiency.

In order to work out these problems, the necessary test equipment first had to be created in which connection the experiments at the required high rotor speeds offered particular technical difficulty. The test rig constructed in 1927 for these investigations has proved satisfactory in every respect and with several supplementary fittings is still in use today.

At the same time another test rig was constructed intended for detailed investigations on certain particular blower impellers at lower rotor speeds and less power. This latter blower test rig is shown in figure 1 in simplified cross section. An iron frame resting on three trestles supports the two-part housing designed for a rotor of 300-millimeter outside diameter, the metering constriction, the throttle mechanism at the outlet end of the duct for the purpose of producing various operating conditions, and the direct-current motor, which is cradled to allow measurement of torque. An electromagnetic control device operates a stop watch for determining rotor speed. The current necessary for operation during an experiment is drawn from a Ward-Leonard system.

Figure 2 shows a simplified cross section of the test rig for experimental impellers designed for very high rotor speeds. The impellers generally have a diameter of 150 to 200 millimeters and may be tested with this rig in one- and two-stage arrangements, at rotor speeds up to about 33,000 rpm, and with variable air densities.

The drive is by a cradled compressed-air turbine, which is designed for an output of about 70 kilowatts at 30,000 rpm. (High-speed electric motors of this power were not available at that time.) The closed-circuit air passage contains the test-section proper with the taps for taking pressures and also the gate valve for producing the various operating conditions. A special arrangement for the reduction of bearing friction permits measuring the torque transmitted by the turbine with an accuracy of $\pm 0.5 \cdot 10^{-3}$ meter kilograms. For measuring the rotor speed there is a calibrated tachometer connected to the blower shaft by a worm drive, as well as a speed-measuring apparatus controlled by a photocell.

Whereas on the low-power test rig a given set of operating constants can be maintained over as a long a period of operation as desired, with the supercharger test rig the periods available for measurements are relatively limited due to decreasing pressure in the compressed-air tank and in some degree also to consideration for the bearings. Under these circumstances, in order to insure a simultaneous reading of all measuring instruments the manometer, tachometer, and dynamometer readings at each stage of a test were photographically recorded.

III. Results of the Experiments:

In order that the air quantities delivered and the pressure rise produced may be indicated independently of rotor dimensions or air density, the results of the measurements will be given in nondimensional parameters as is customary (reference 2).

Let

d_a = outside diameter of rotor = inside diameter of housing (clearance = 0)

d_1 = hub diameter of rotor

F = air-flow cross-sectional area = $(d_a^2 - d_1^2)\frac{\pi}{4}$

u_a = peripheral speed = $\frac{d_a \pi n}{60}$

G = weight of air flowing per second

Q = volume of air flowing per second = $\frac{G \cdot R \cdot T}{p}$

k = ratio of specific heats for constant pressure and for constant volume $\frac{c_p}{c_v}$

The subscript I denotes the gas as it existed in a state of rest before entrance into the blower and the subscript II, after exit from the blower and once again in a state of rest.

The useful work of the blower

$$N = \int_I^{II} Q dp$$

for adiabatic compression amounts to

$$N_{ad} = \frac{k}{k-1} Q_I \cdot p_I \left[\left(\frac{p_{II}}{p_I} \right)^{\frac{k-1}{k}} - 1 \right] \tag{1}$$

or for each kilogram of air flowing through per second

$$\frac{N_{ad}}{G} = H_{ad} = \frac{k}{k-1} R \cdot T_I \left[\left(\frac{p_{II}}{p_I} \right)^{\frac{k-1}{k}} - 1 \right] \tag{2}$$

with $p_{II} = p_I + \Delta p$, from equation (1) by series development is obtained

$$N_{ad} = Q_I \cdot \Delta p \left[1 - \frac{1}{2!k} \frac{\Delta p}{p_I} + \frac{k+1}{3!k^2} \left(\frac{\Delta p}{p_I} \right)^2 - \frac{(k+1)(2k+1)}{4!k^3} \left(\frac{\Delta p}{p_I} \right)^3 + \cdots \right] \tag{3}$$

For a value of $K = 1.4$ this gives

$$N_{ad} = Q_I \cdot \Delta p \left[1 - 0.3571 \frac{\Delta p}{p_I} + 0.2041 \left(\frac{\Delta p}{p_I} \right)^2 - 0.1385 \left(\frac{\Delta p}{p_I} \right)^3 + \cdots \right] \tag{3a}$$

For small values of $\frac{\Delta p}{p_I}$ the terms of higher order may be omitted and then the effective work for an incompressible flow is obtained

$$N_{ink} = Q_I \cdot \Delta p \tag{4}$$

It follows from equations (3) and (4) that for a pressure rise $\Delta p = 0.1\ p_I$ the omission of the terms of higher order would give an effective work value about 3.4 percent too high and a correspondingly overestimated efficiency. For $\Delta p = 0.05\ p_I$ the error would be about 1.7 percent and for $\Delta p = 0.01\ p_I$ about 0.4 percent.

The work absorbed is determined in both test rigs from the moments of reaction of the cradled driving motors; the expenditure of work necessary to cover mechanical losses is determined by a special series of measurements. As a control on the work measurements, the temperatures ahead of and behind the compressor are measured in the tests on the high-speed rig. If L denotes the work absorbed less the deduction for mechanical losses and T_{IIad} denotes the final temperature corresponding to an adiabatic compression, then the temperature-rise adiabatic efficiency is

$$\eta_{iad} = \frac{N_{ad}}{L} = \frac{T_{IIad} - T_I}{T_{II} - T_I} \tag{5}$$

The flow coefficient φ and the pressure coefficient ψ are used as nondimensional characteristics. The flow coefficient φ_I is the ratio of the axial-flow velocity of the gas to the peripheral velocity of the rotor; it is referred to as the initial state of rest of the intake air (condition I). It is thus

$$\varphi_I = \frac{G \cdot R \cdot T_I}{p_I \cdot F \cdot u_a} \tag{6}$$

The pressure coefficient ψ_I is the ratio of the pressure rise produced by the compressor to the dynamic pressure corresponding to the peripheral speed at the density of condition I; it is

$$\psi_I = \frac{\Delta p}{\frac{\rho_I}{2} \cdot u_a^2} \tag{7}$$

In the designing of multistage compressors, the use of this equation for the pressure ratio results in certain mathematical inconvenience; hence for practical purposes the pressure ratio calculated on the work of adiabatic compression per kilogram per second of weight of air flow is used.

$$\psi = \frac{H_{ad}}{\frac{u_a^2}{2g}} \tag{8}$$

From equations (2), (7), and (8) there follows the relation between ψ and ψ_I:

$$\psi = \psi_I \frac{k}{k-1} \frac{p_I}{\Delta p} \left[\left(\frac{p_{II}}{p_I} \right)^{\frac{k-1}{k}} - 1 \right] \tag{9}$$

Letting $p_{II} = p_I + \Delta p$, from equation (9) by series development and with $k = 1.4$, as in equations (3) and (3a), is obtained

$$\psi = \psi_I \left[1 - 0.3571 \frac{\Delta p}{p_I} + 0.2041 \left(\frac{\Delta p}{p_I} \right)^2 - 0.1385 \left(\frac{\Delta p}{p_I} \right)^3 + \ldots \right] \ldots \tag{10}$$

In equation (10)

$$\frac{\Delta p}{p_I} = \psi_I \frac{u_a^2}{2g} \frac{1}{RT_I} \tag{11}$$

For small values of $\frac{\Delta p}{p_I}$, the terms of higher order may be omitted and $\psi = \psi_I$ may be set.

With respect to the older tests, all evaluations in this report are based on the pressure coefficient ψ_I. The relation between ψ and ψ_I is shown in figure 3 for various peripheral speeds and temperatures. The measurements were in general made at an inlet temperature of approximately 305° K.

Figure 4 gives the measurements obtained on a one-stage blower (built in 1927) at low rotor speeds. At the upper left of the figure, a one-stage installation consisting of a 12-blade rotor, an 11-blade inlet stator, and a 13-blade outlet stator is drawn to a

relative scale in terms of the tip diameter. The blade spacing in the plan view corresponds to a developed section at hub diameter; for other blade sections the blade spacing is to be understood as larger in proportion to the diameter of the respective cylindrical sections.

Below this the rotor blade is again laid out to a larger scale to show hub, center, and tip sections. In this drawing the cylindrical sections[1] have been presented as parallel plane sections to facilitate determining intermediate blade sections from them.

At the upper right of the figure the pressure coefficient ψ_I and the temperature-rise adiabatic efficiency η_{iad} have been plotted against the flow coefficient φ_I, the values being those found by observations at 1000, 2000, and 3000 rpm. The Reynolds number, calculated from the velocity of the air relative to the blade tip, was approximately $2 \cdot 10^5$.

The results of measurement in the high rotor-speed range, with peripheral speeds between approximately 150 and 200 meters per second are given in figures 5 and 6. Proportions and blade sections of this blower, made on a smaller scale for tests in the high-speed test rig, are the same as those of figure 4.

The change in the shape of the performance curve with a change of the Mach number may be clearly seen in figure 5. As the rotor speed increases, the curve becomes more nearly vertical and the maximum value of the flow coefficient is lowered; at the lower flow-coefficient values within the normal working range, higher pressure ratios are obtained at the same flow ratio as the Mach number increases. At the rotor speeds given in the figure, the Mach numbers computed on the relative flow velocity at the blade tips in the range of best efficiencies are 0.45, 0.60, 0.72, and 0.80.

Figure 6 shows the behavior of the blower with alteration of the air density. The curve given in figure 5 for 30,000 rpm is transferred to figure 6; it is the curve for an inlet pressure of

---

[1] For the manufacture of the relatively small experimental blades photographs of large-scale blade-section drawings were used at the Aerodynamic Experimental Institute instead of working from numerical coordinates.

1 atmosphere. It is clear from the figure that even with a substantial change in the inlet pressure such as is caused, for example, by the throttling down of the inlet flow, which is necessary in test rigs with low-powered drives, the test results are independent of inlet pressure within the limits of accuracy of the measurements. In the neighborhood of the maximum flow coefficient, the measurements obtained at the lowest absolute inlet pressure, namely 0.25 atmosphere, are shifted in the direction of smaller flow ratios.

The design and performance of a blower intended for about one-half the air delivery of the type just discussed is shown in figures 7 and 8. Proportions and blade sections for both sizes of impellers are shown in figure 7. The data obtained from the low-speed tests are shown in figure 7 and those of the high-speed tests in figure 8. Reynolds number and Mach numbers are of the same magnitude as those given in connection with figures 4 and 5.

Figures 9 to 12 show the proportions, blade sections, and performance charts of two blowers designed for values of the flow ratio intermediate to those of the two first-mentioned blower types. The installations shown in figures 9 and 11 and the blade sections at hub and tip also shown are drawn in the form of two-stage models. In the performance curves of figures 10 and 12 the pressure coefficient is in each case calculated on a one-stage basis. The Mach numbers (see the text pertaining to fig. 5) for the rotor speeds indicated in these charts and in the region of highest efficiency values are approximately 0.50, 0.63, and 0.75.

Figures 13 and 14 give the data for a blower of larger air output. From the proportions shown in figure 13, there results a relatively great axial dimension for this type of impeller, so that it was not used for multistage installations. In like manner as for the two first-mentioned one-stage blowers, the data obtained at low rotor speeds are given in figure 13 and at the higher rotor speeds in figure 14. For the latter the Mach numbers are 0.38, 0.47, and 0.56.

In figures 15 and 16 are given the particulars of a one-stage blower designed for axial inlet using no forward stator. As an installation of the blower without an outlet stator was also required for a special purpose, the data obtained from this latter installation are shown in figure 15 along with the characteristic curve obtained for normal blade angle and using the outlet stator. In figure 16 are shown the performance curves of the blower using the outlet stator and with various blade angles. In this figure, which

shows the ranges of pressure coefficient and flow coefficient for seven different blade angles, curves of equal efficiencies have been included. At steeper blade angles greater pressure and flow coefficients are obtained. The operating point, which was made the basis of the 24° blade-angle design, lies within the region of the highest efficiencies measured. The absolutely highest value of efficiency on the graph corresponds to a somewhat flatter blade angle.

IV. Remarks on the Design of Blowers:

As a very general observation, it may be said that the dimensions of a blower will be smaller in proportion as the flow coefficient and pressure coefficient for which it is designed - within the range of the chosen performance curve - are greater. (See equations (6) to (8).) However, impellers of small flow coefficient are also indispensable when, due to limitations of the power source, only a relatively low rotor speed is permissible and at the same time relatively small quantities of air are to be pumped. Low rotor speeds require necessary large outside diameters in order to attain high peripheral speeds; on the other hand, a large flow coefficient when only a small quantity of air was required would lead to very small cross sections, and thereby at large diameters would result in very short blade lengths and a corresponding drop in efficiency. However, it must be noted that with a low flow coefficient, the desired high pressure ratio can only be attained with some difficulty.

As for the design of a blower impeller itself, if measurements of proposed blade sections taken in cascade arrangement are available, the lift and the drag coefficients on the cascade basis may be used directly; otherwise, proceeding from the measurements made on a single blade, the attempt must be made to determine the coefficients for the cascade arrangement by computation. (See reference 3.) Another procedure, which is generally chosen in the Göttingen Institute, is to try by reshaping the blade to attain the same coefficients for each blade when in cascade as were determined for the single blade by itself. (See reference 4.) In connection with these questions it may be remarked that many publications are available on the subject of the computation and design of axial blowers (among which are the works of Ackeret, Betz, Eck, Keller, Traupel, and Weinig), to which, however, detailed reference cannot be made within the limits of this report.

In blower design, generally speaking, the determination of the blade sections should not be undertaken on the basis of the maximum lift coefficients, for they must be selected for operation at a

middle point of the performance curve, which will be the normal operating point of the impeller at the highest possible efficiency. This is necessary because if in operation the flow volume is throttled down, there will arise greater angles of incidence at which the impeller must still be able to work with good efficiency. Furthermore, at lower inlet temperatures and corresponding higher Mach numbers, substantially smaller maximum lift values will be attained under certain circumstances. However, for practical purposes, excessive coefficients of lift will be chosen for the hub region so that the blade chord in that region can be kept within permissible limits.

The direction of inflow plays an important part in the design of the rotor itself. By means of the stator preceding it, the air may be introduced in a direction agreeing with the rotor spin or in a direction counter to it; or, with omission of the stator altogether, the air may be introduced axially. A higher peripheral speed is made possible while maintaining a prescribed incident air velocity relative to the rotor blades if the design is for inflow in the direction of rotor spin. By designing for inflow in the opposite direction, good pressure ratios can be obtained even with a relatively small hub diameter, whereas otherwise a greater hub diameter would have to be used. Because in blowers in which the inflow is turned counter to the rotor spin, the static-pressure rise is created principally in the rotor; if the inflow whirl is in the same direction as rotor spin, the rotor will operate with smaller reaction due to the greater whirl in the outflow and consequently will give less axial thrust.

Translation by Edward S. Shafer,
National Advisory Committee
for Aeronautics.

REFERENCES

1. Betz, A.: Axiallader. Jahrb. 1938, d. D. Luftfahrtforschung, Lilienthal-Gesellschaft f. Luftfahrtforschung, Berlin, R. Oldenbourg (München), pp. II 183-II 186. (NACA TM No. 1073, 1944.)

2. Regeln für Leistungsversuche an Verdichtern. VDI - Verlag.

3. Schilhansl, M.: Näherungsweise Berechnung von Auftrieb und Druckverteilung in Flügelgittern. Jahrb. 1927 d. WGL, R. Oldenbourg (München), pp. 151-167.

4. Betz, A.: Diagramme zur Berechnung von Flügelreihen. Ing.-Archiv., Bd II, Heft 3, Sept. 1931, pp. 359-371. (NACA TM No. 1022, 1942.)

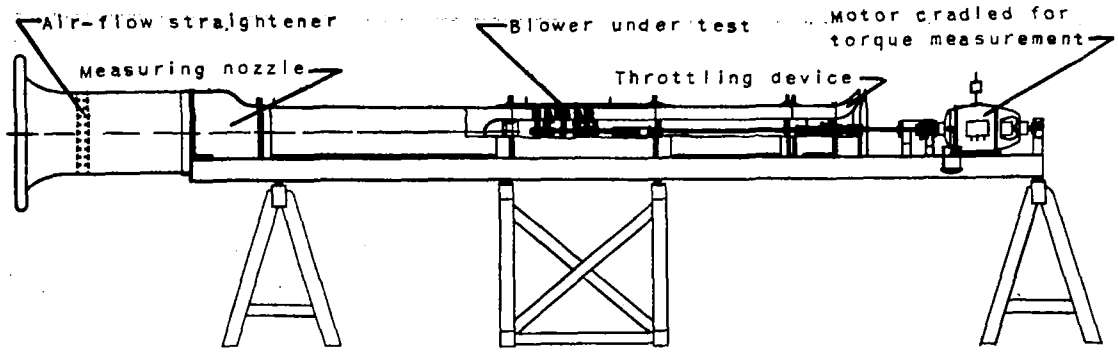

Figure 1. - Blower test rig.

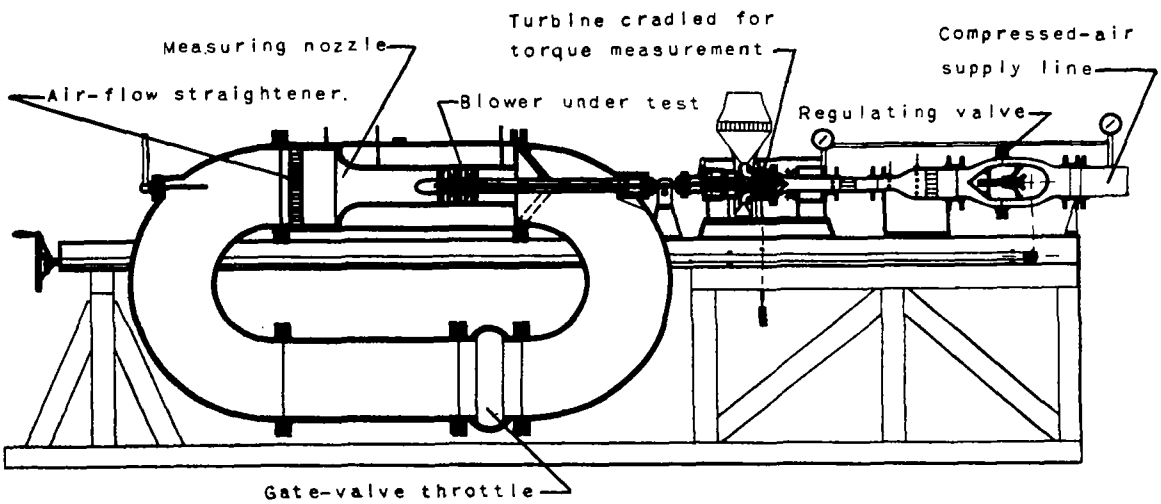

Figure 2. - Compressor test rig.

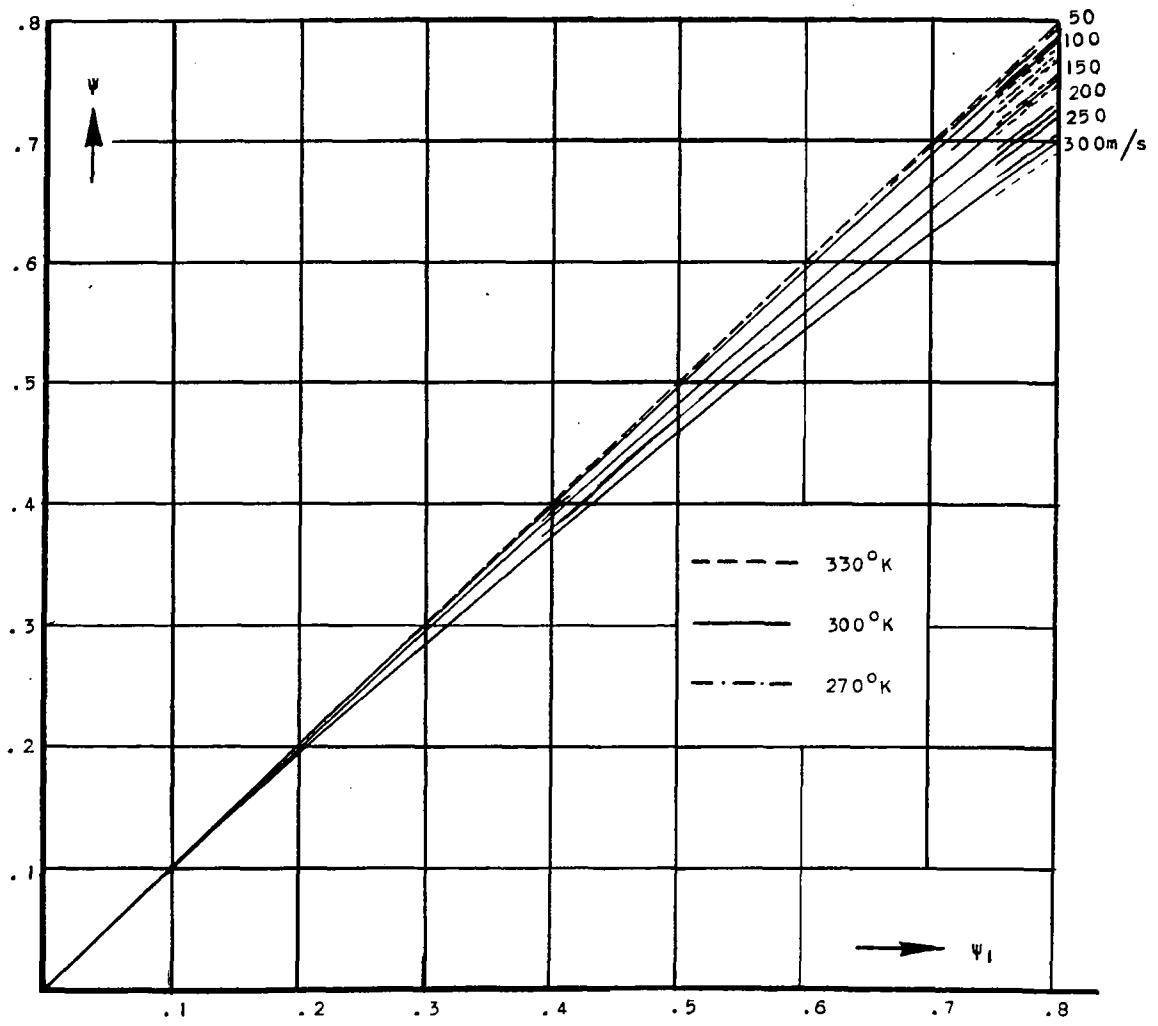

Figure 3. - Pressure coefficient ψ plotted against pressure coefficient ψ_1.

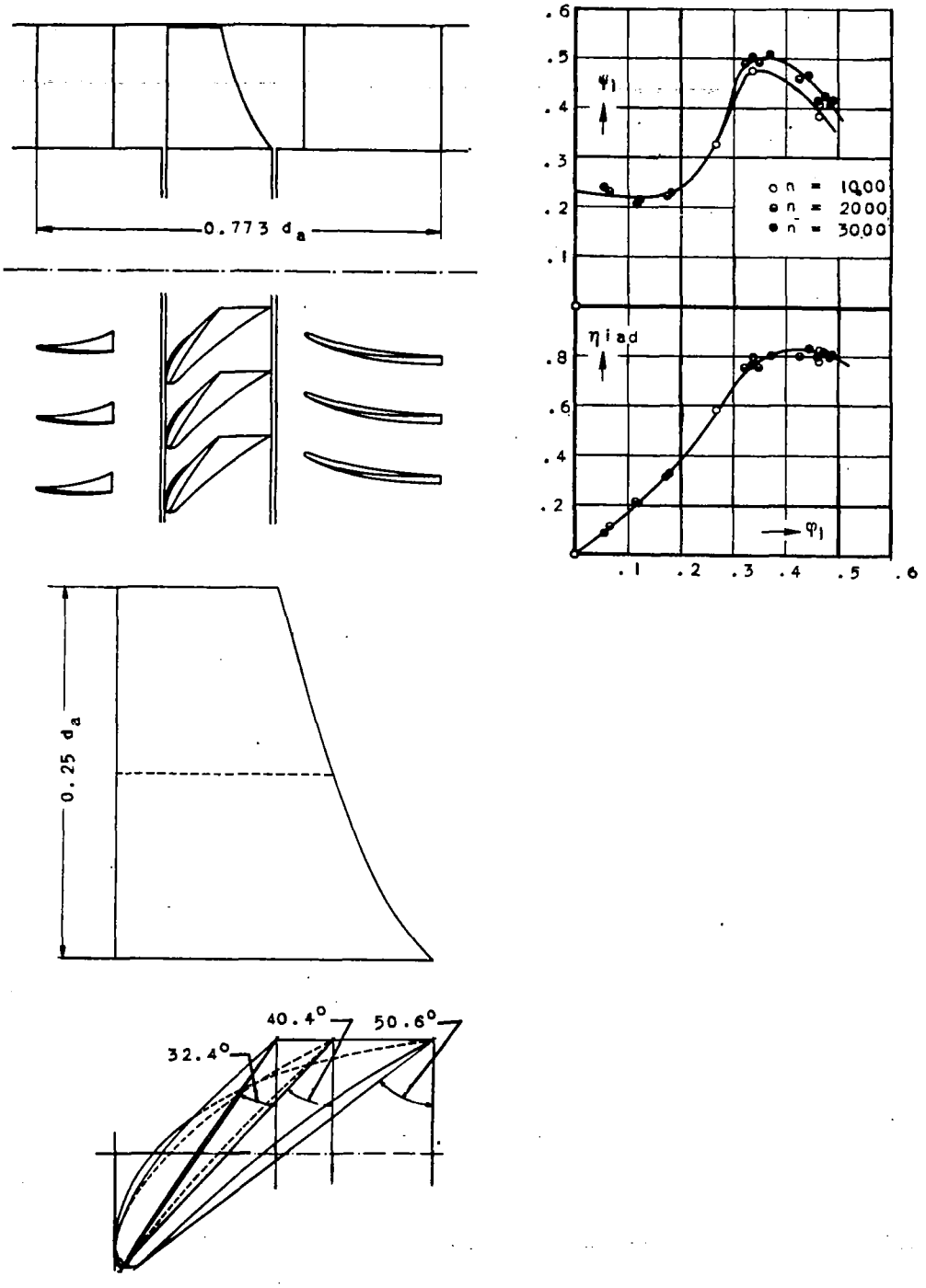

Figure 4. - 12-bladed rotor 706. Outside diameter d_a, 300 millimeters; inside diameter d_i, 150 millimeters; peripheral speed u_a, 47.1 meters per second; rotor speed n, 3000 rpm; 11-bladed inflow stator; 13-bladed outflow stator.

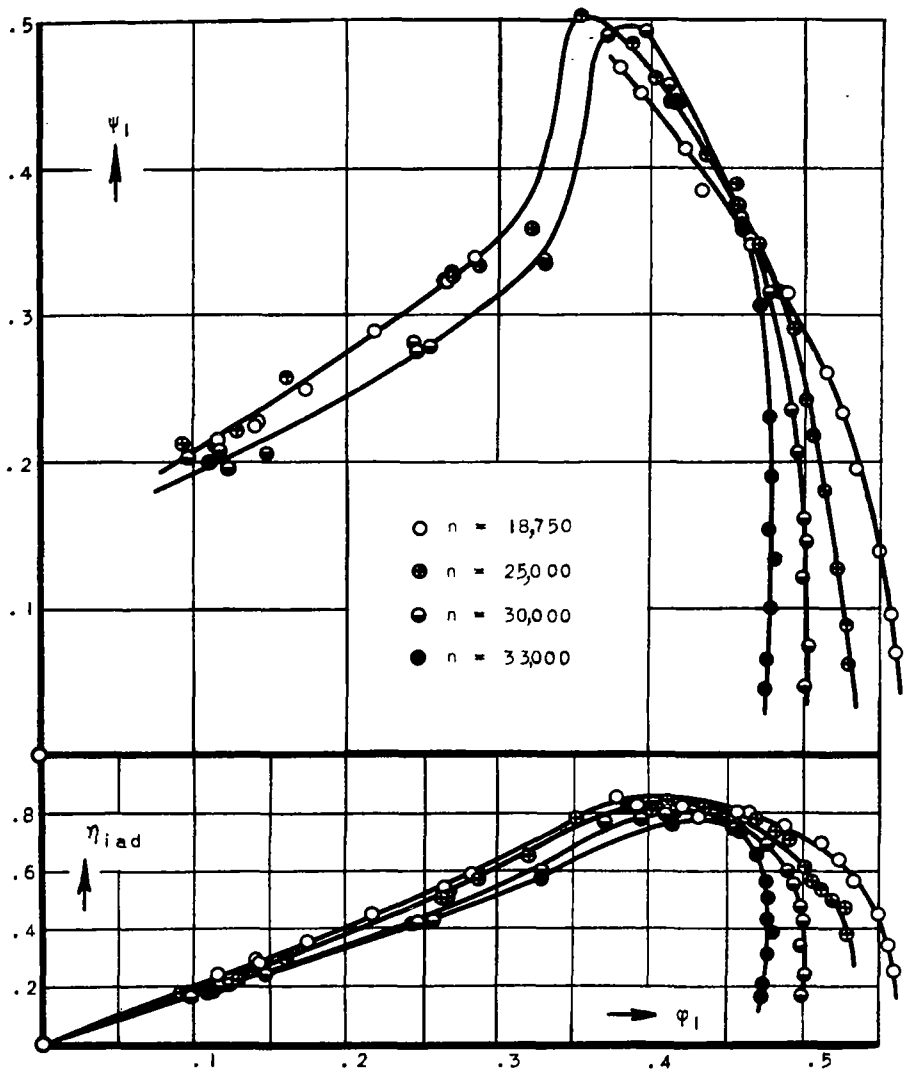

Figure 5. - 12-bladed rotor 866. Outside diameter d_a, 150 millimeters; inside diameter d_i, 75 millimeters; peripheral speed u_a, 235.6 meters per second; rotor speed n, 30,000 rpm; 11-bladed inflow stator; 13-bladed outflow stator.

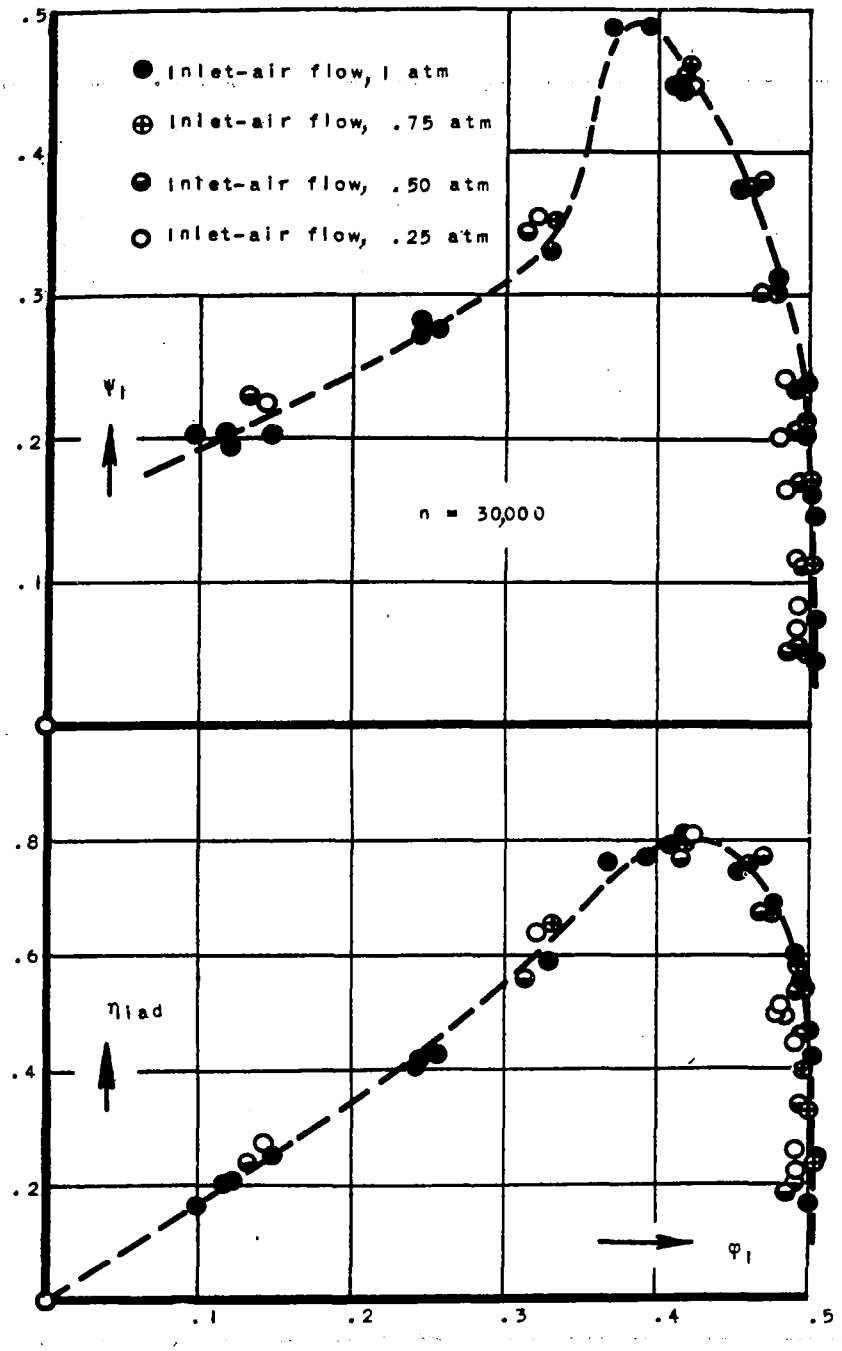

Figure 6. - Behavior of the blower under variation of the air density.

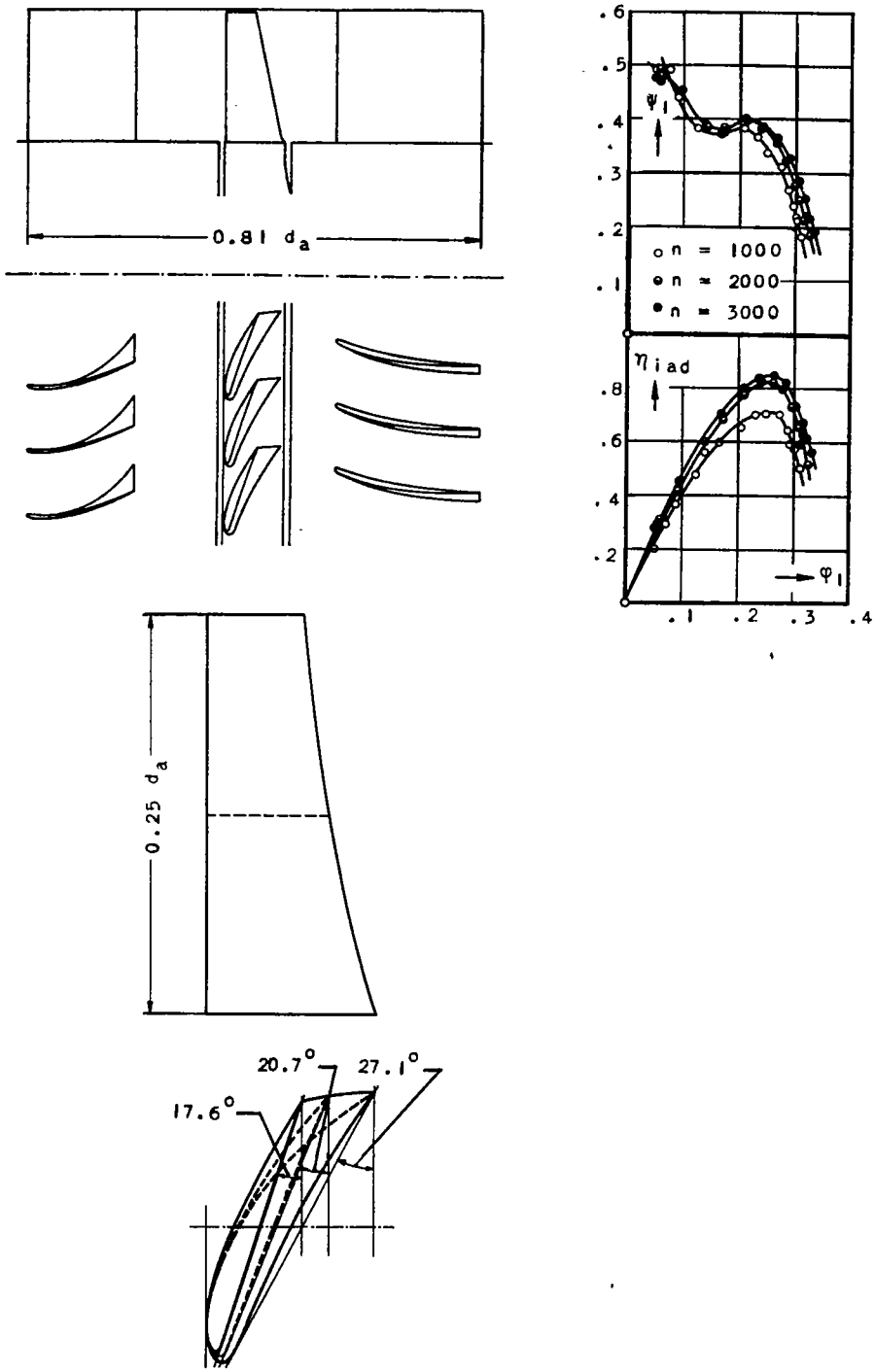

Figure 7. - 12-bladed rotor 998. Outside diameter d_a, 300 millimeters; inside diameter d_i, 150 millimeters; peripheral speed u_a, 47.1 meters per second; rotor speed n, 3000 rpm; 13-bladed inflow stator; 13-bladed outflow stator.

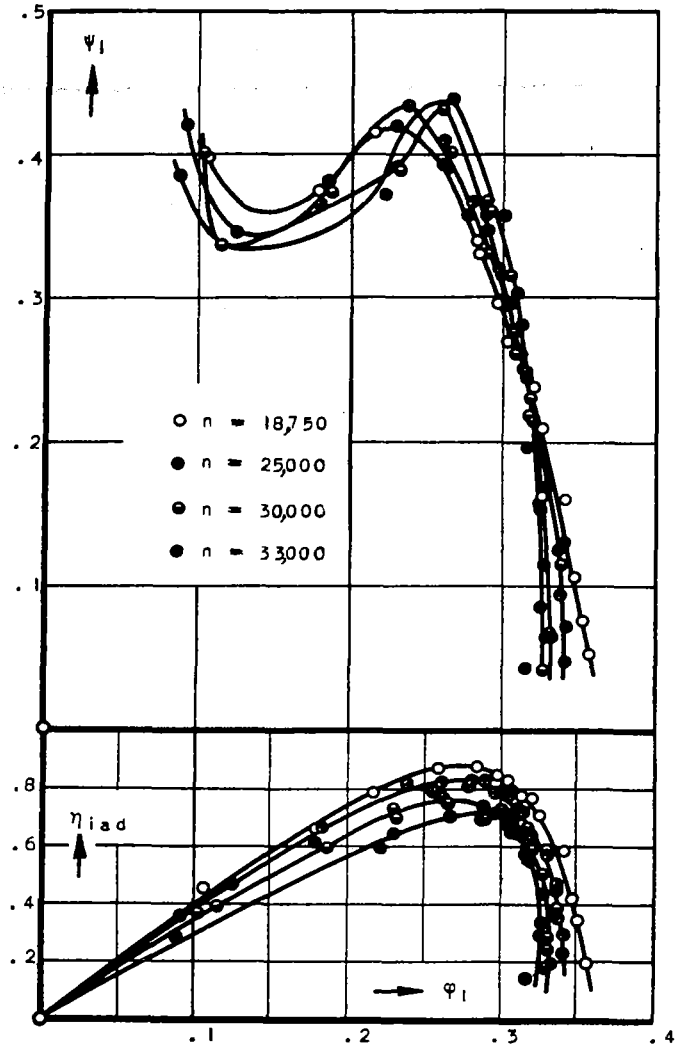

Figure 8. - 12-bladed rotor 1115. Outside diameter d_a, 150 millimeters; inside diameter d_i, 75 millimeters; peripheral speed u_a, 235.6 meters per second; rotor speed n, 30,000 rpm; 13-bladed inflow stator; 13-bladed outflow stator.

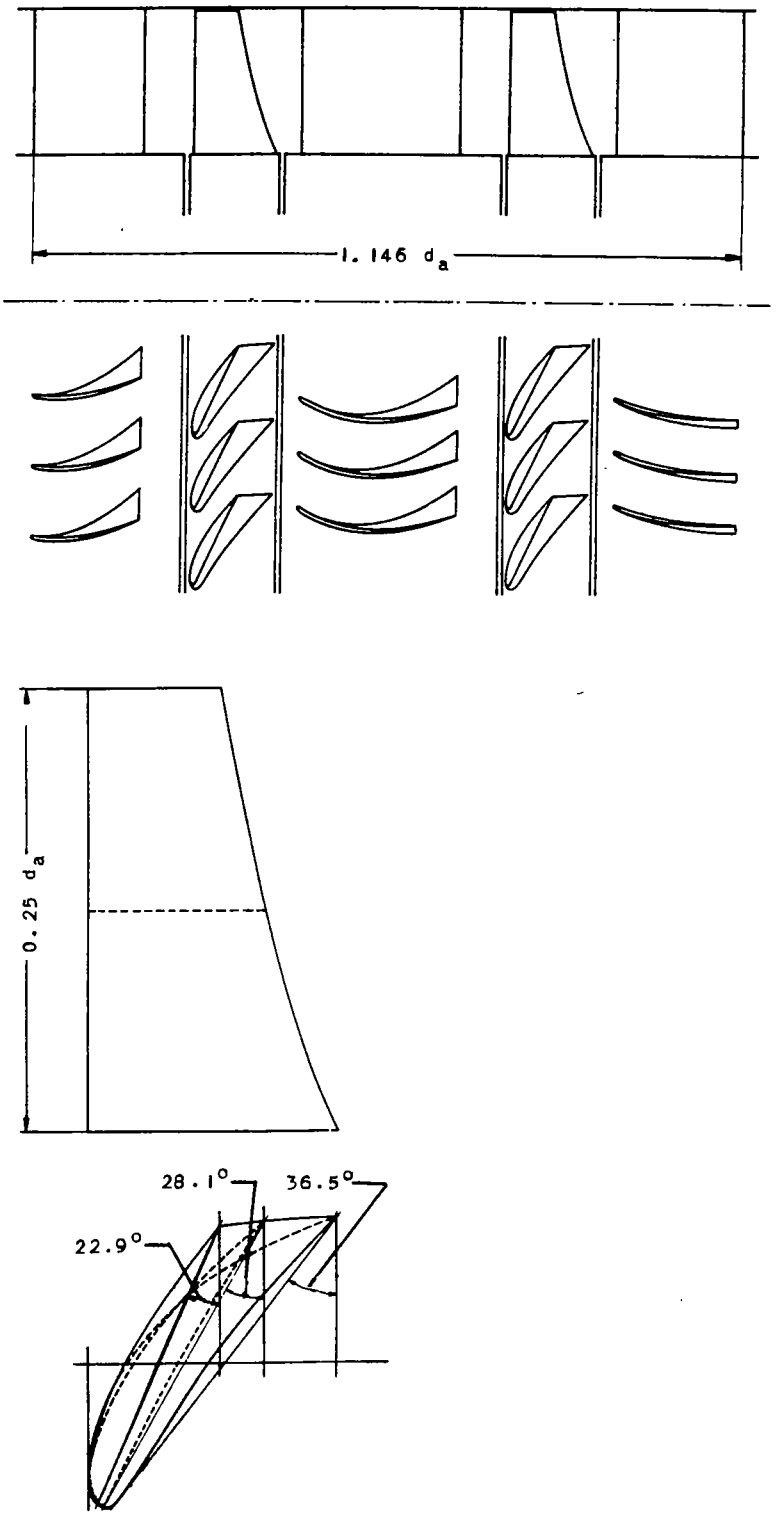

Figure 9. - Proportions and blade sections. 12-bladed rotor E68; 13-bladed inflow stator; 17-bladed intermediate stator; 17-bladed outflow stator.

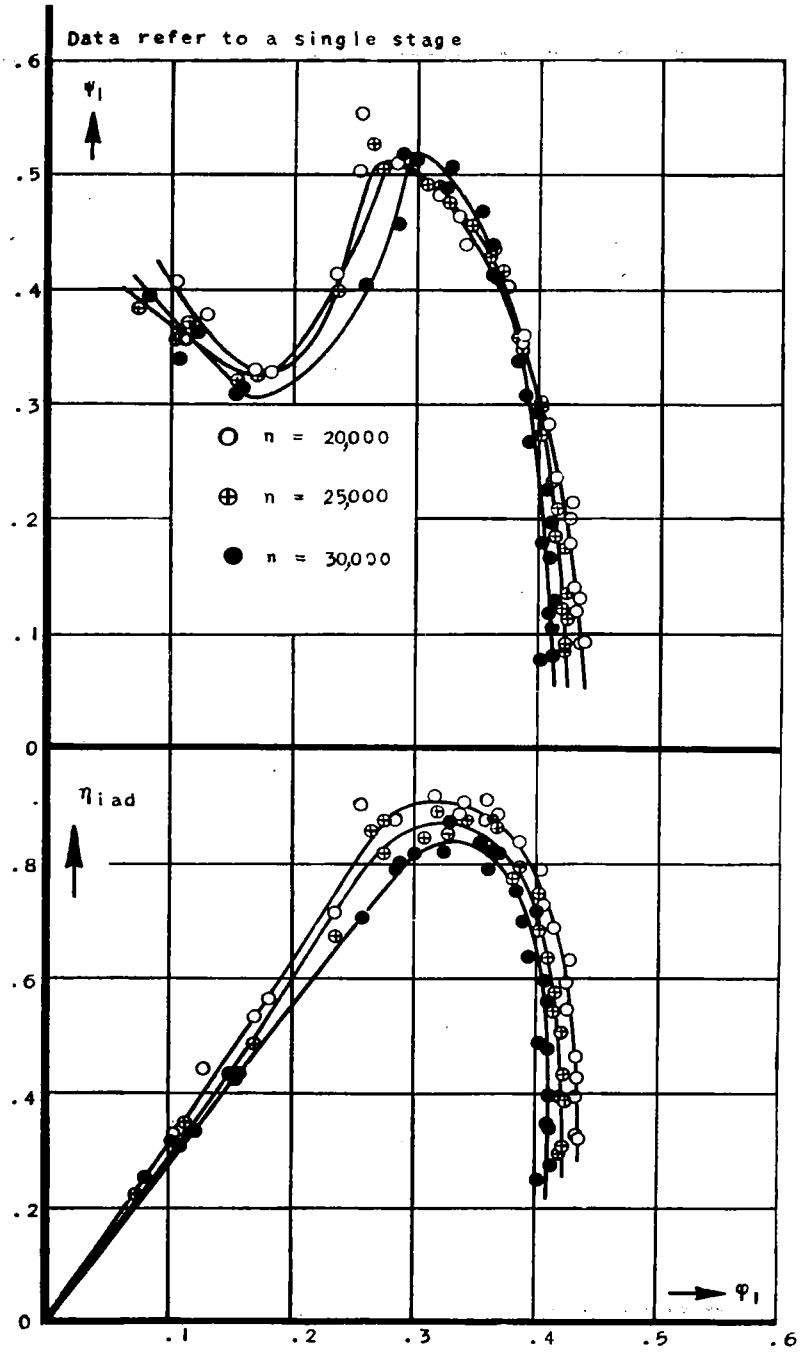

Figure 10. - Performance chart of single-stage blower using rotor E68 of figure 9. Outside diameter d_a, 150 millimeters; inside diameter d_i, 75 millimeters; peripheral speed u_a, 235.6 meters per second; rotor speed n, 30,000 rpm.

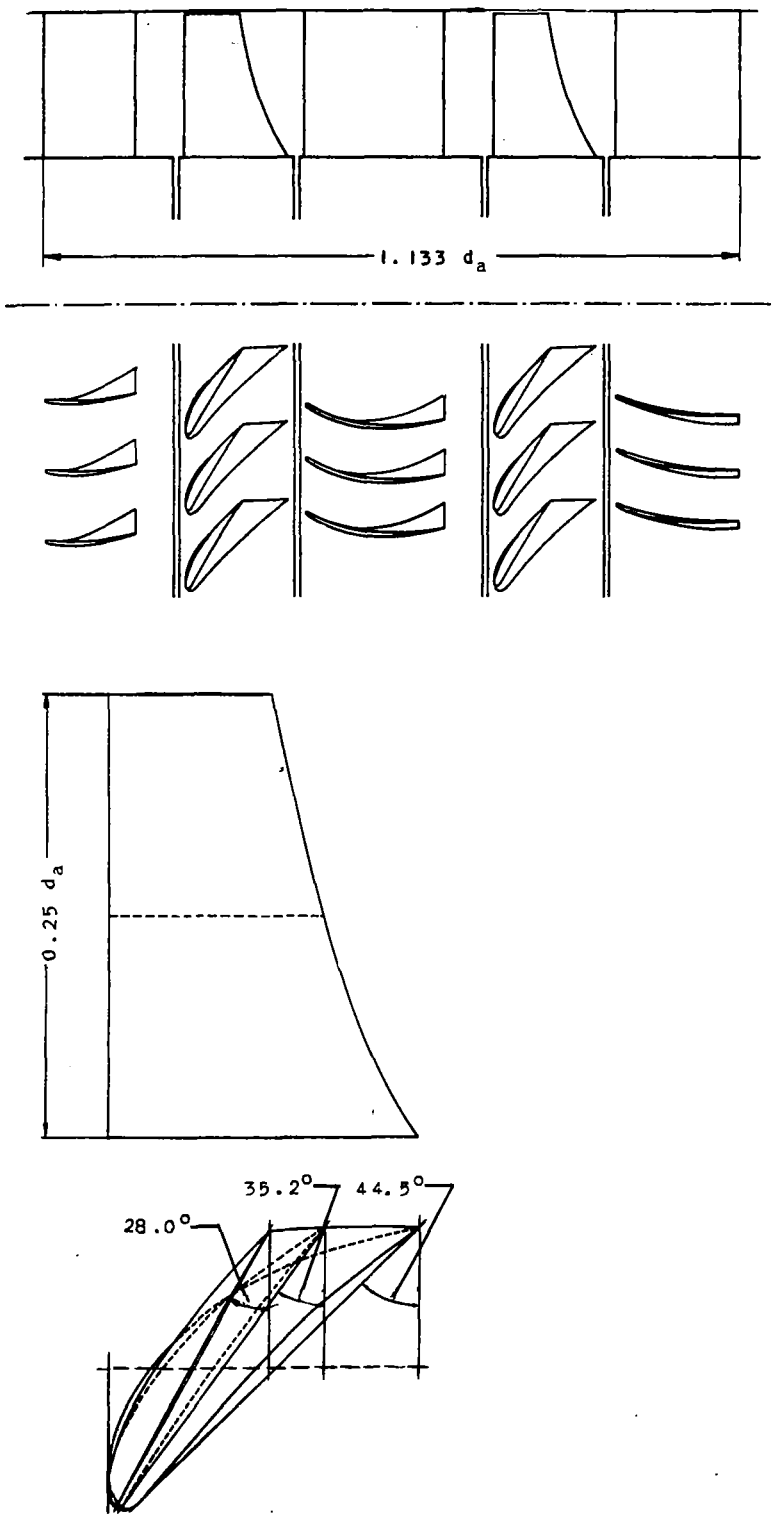

Figure 11. - Proportions and blade sections. 12-bladed rotor E-78; 13-bladed inflow stator; 17-bladed intermediate stator; 17-bladed outflow stator.

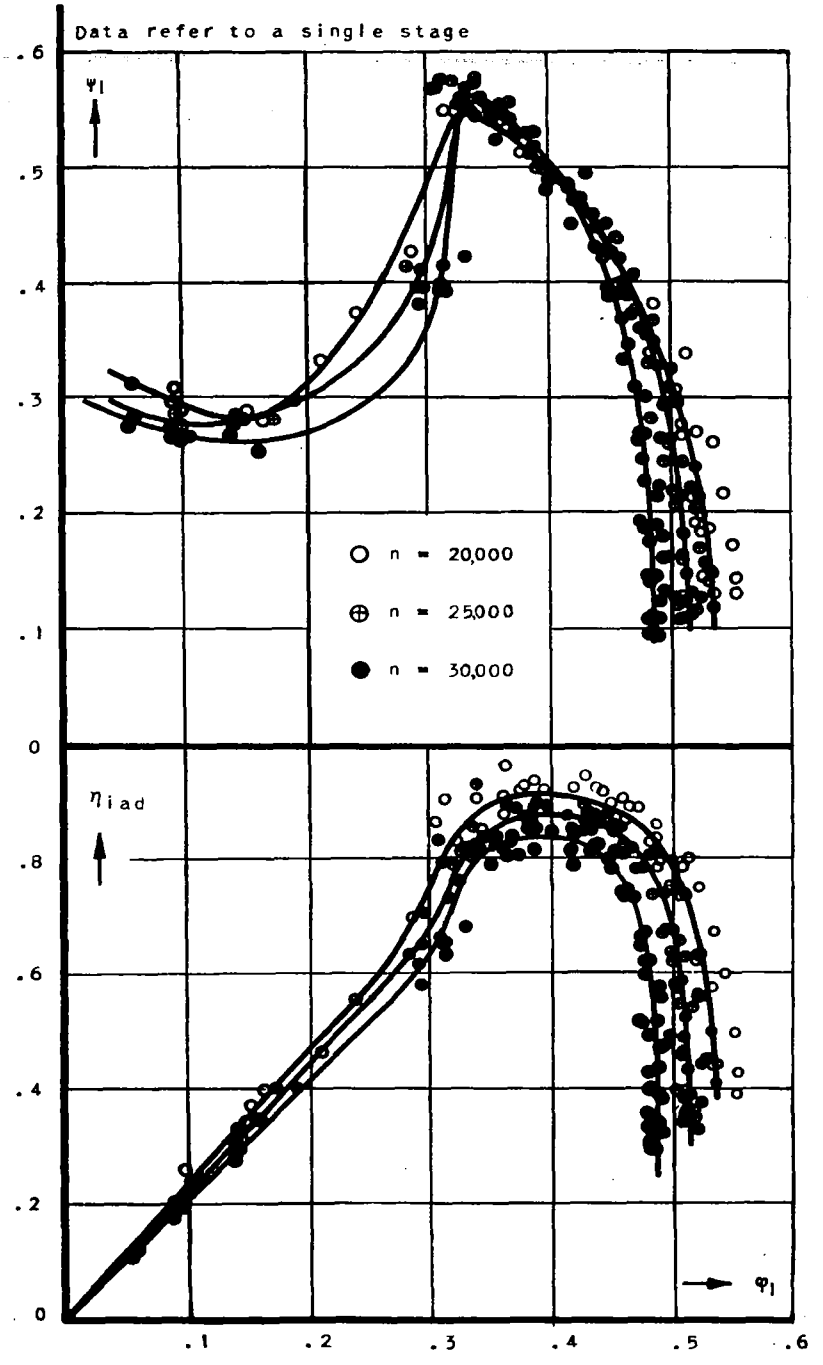

Figure 12. - Performance chart of single-stage blower using rotor E78 of figure 11. Outside diameter d_a, 150 millimeters; inside diameter d_i, 75 millimeters; peripheral speed u_a, 235.6 meters per second; rotor speed n, 30,000 rpm.

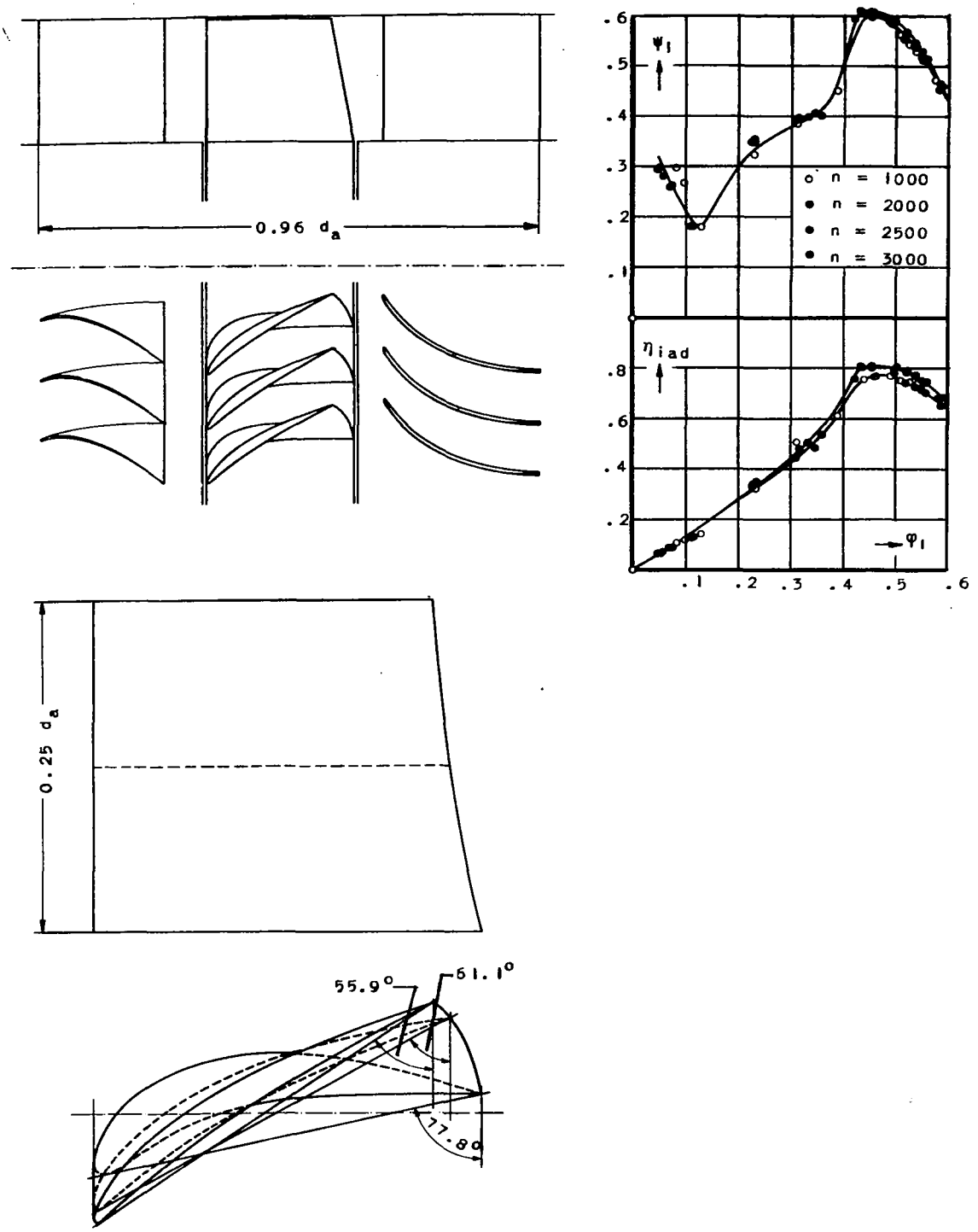

Figure 13. - 14-bladed rotor 871. Outside diameter d_a, 300 millimeters; inside diameter d_i, 150 millimeters; peripheral speed u_a, 47.1 meters per second; rotor speed n, 3000 rpm; 13-bladed inflow stator; 15-bladed outflow stator.

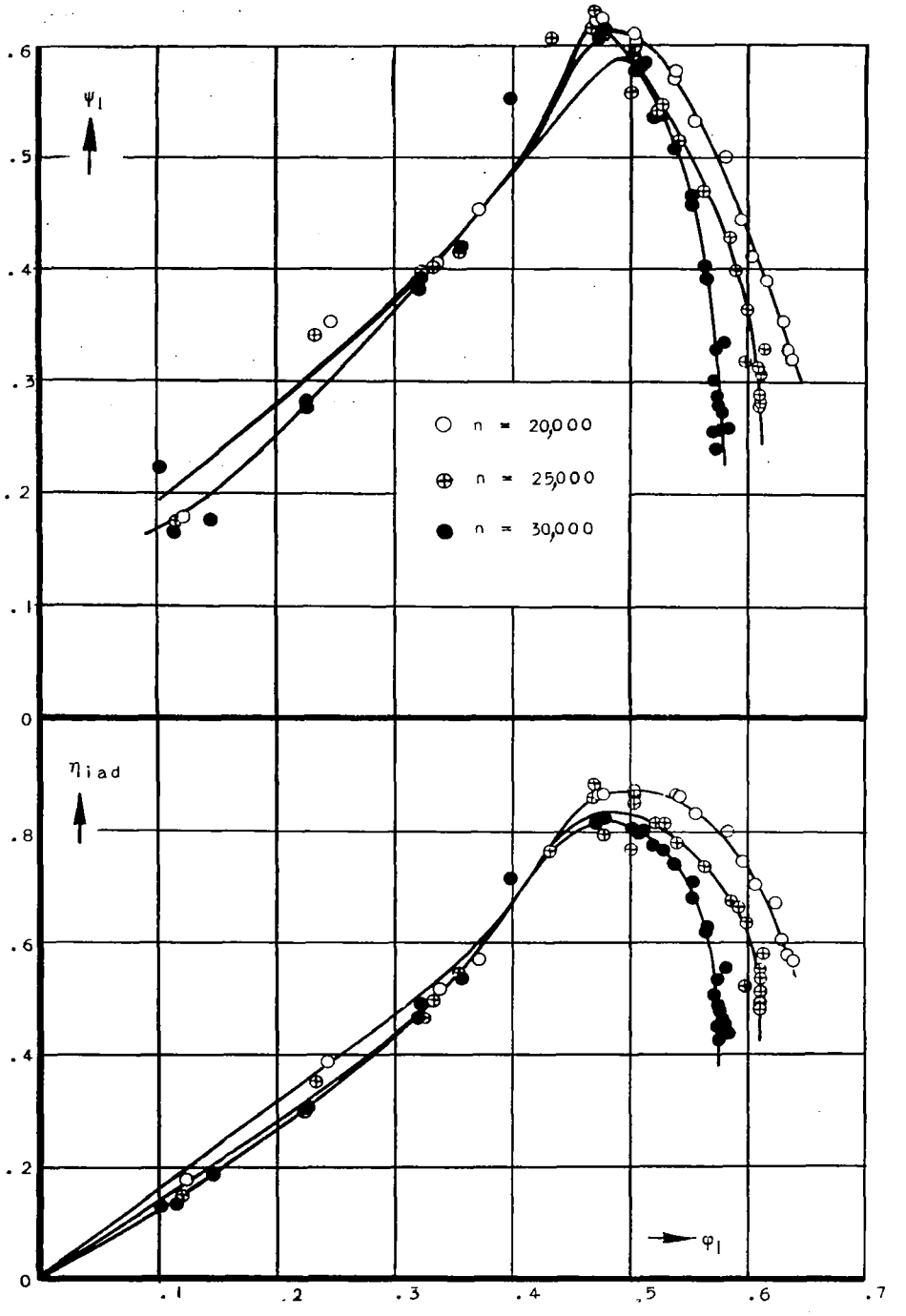

Figure 14. - 14-bladed rotor E118. Outside diameter d_a, 150 millimeters; inside diameter d_i, 75 millimeters; peripheral speed u_a, 235.6 meters per second; rotor speed n, 30,000 rpm; 13-bladed inflow stator; 15-bladed outflow stator.

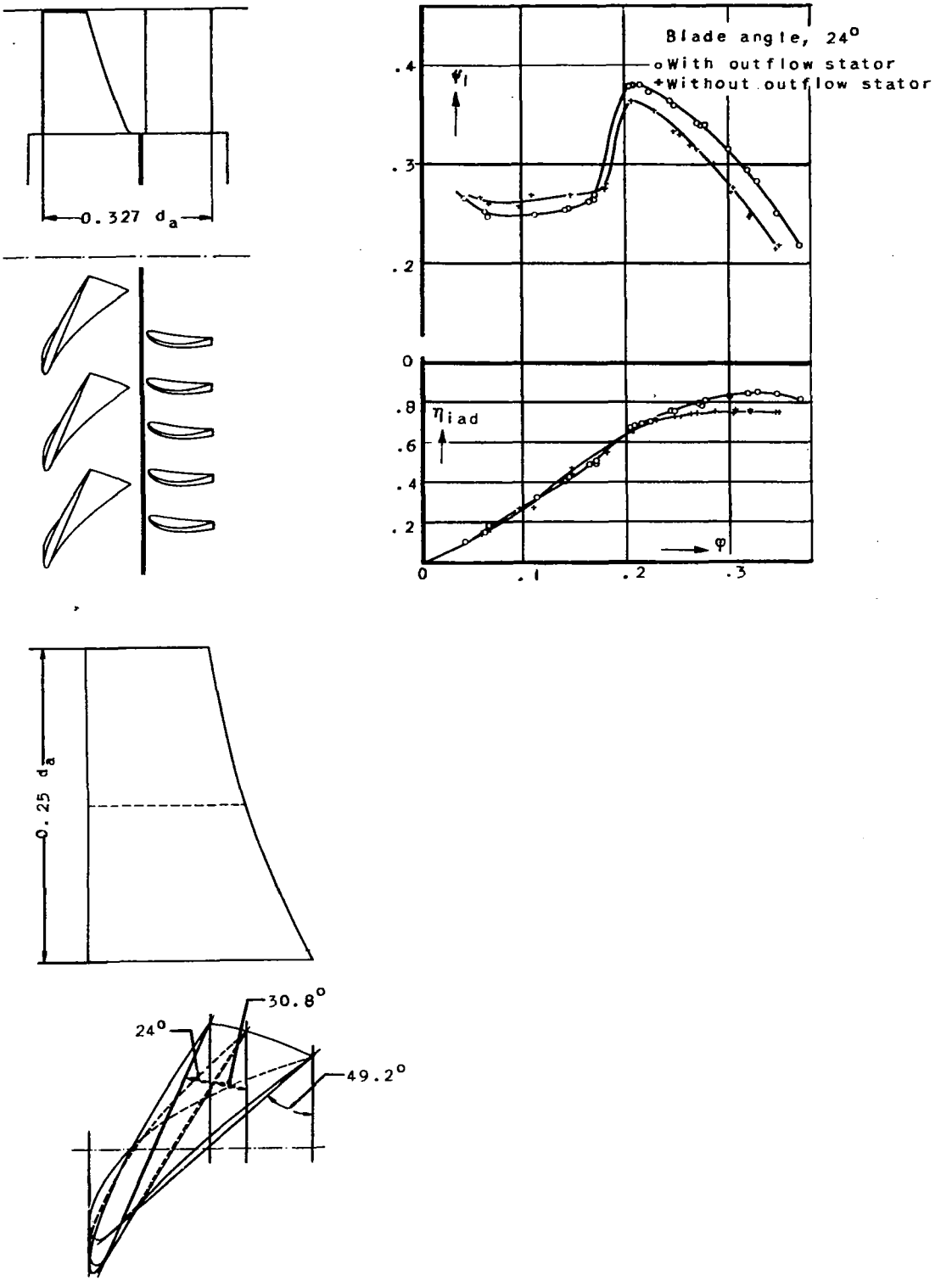

Figure 15. - 8-bladed rotor E191. Outside diameter d_a, 300 millimeters; inside diameter d_i, 150 millimeters; blade angle, 24°; peripheral speed u_a, 47.1 meters per second; rotor speed n, 3000 rpm; 17-bladed outflow stator.

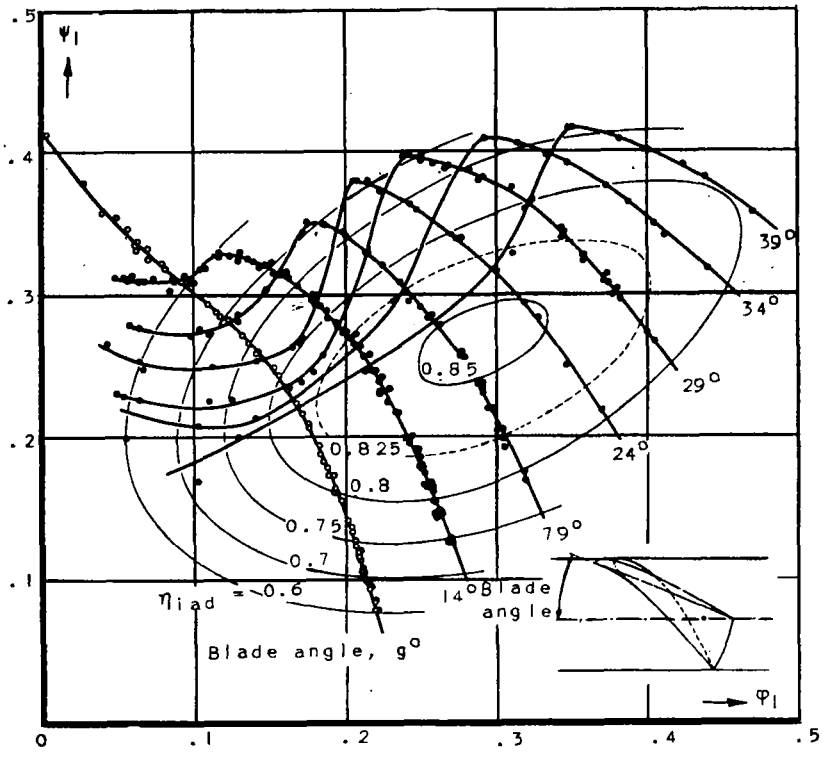

Figure 16. - 8-bladed rotor E191, as shown in figure 15. Blade angle, 9° to 39°.

NASA Technical Library
3 1176 01441 2291